

Diffraction in resonant electron scattering from helical macromolecules: Effects of the DNA backbone

Laurent Caron* and Léon Sanche

Groupe de Recherches en Sciences des Radiations, Faculté de médecine, Université de Sherbrooke, Sherbrooke, QC J1H 5N4, Canada

(Received 14 June 2005; published 26 September 2005)

We recently developed a theoretical framework to treat low-energy electron scattering from helical macromolecules. In this article, we use this framework to extend our previous model of simple base-pair scatterers, organized into the DNA structure, to include the backbone. The internal diffraction pattern due to base pairs is still present, but addition of the backbone screens the base pairs by a factor of 2. More interestingly, the effect of constructive interference on the phosphate groups within the backbone itself is seen to be strong at lower energies. We perform a calculation for electrons incident perpendicular and parallel to the axis of a fragment and find comparable electron patterns on the phosphate groups at the surface of films consisting of vertically or horizontally arranged segments relative to the substrate.

DOI: [10.1103/PhysRevA.72.032726](https://doi.org/10.1103/PhysRevA.72.032726)

PACS number(s): 34.80.Bm, 87.64.Bx

I. INTRODUCTION

Recently, there has been considerable interest in understanding, both at the experimental [1–10] and theoretical [11–19] level, the interactions of low-energy electrons (LEEs) with the DNA molecule and its basic constituents. The major impetus for such investigations has arisen from the important role of LEEs in radiobiology. The ultimate goal of this field is to arrive at a complete description of the effects of ionizing radiation in living cells and organisms by analyzing the sequence of events by which radiation modifies a biological system, and subsequently, by studying the biochemical and biological responses of this system to the transformations. In this sequence, the primary events result from the propagation of the initial high-energy particle or of other fast charged particles produced by the primary radiation (e.g., Compton and photoelectrons). These fast particles produce excited molecules, cations and secondary electrons (SE). The latter contain a major portion of the energy of the primaries [20]. The majority of SE have energies below 30 eV and are produced in large quantities ($\sim 3 \times 10^4/\text{MeV}$) [21,22]. The primary energy deposits are now fairly well understood [23,24] and the available data serve to calculate energy absorption in biological tissue from different types of ionizing radiation [25,26]. There exists, however, a large gap of knowledge between our understanding of these primary events, which determine doses, and the slower chemical events responsible for the products of ionizing radiation [27]. We can determine quite precisely the energy deposited in a given volume of condensed matter but, we do not have a precise understanding and knowledge of the subsequent events, which occur within the femtosecond time scale. As a consequence, there is no well-defined relationship between adsorbed dose and the induced biological effects. To close this gap, it is crucial to understand the interaction of

LEEs with vital cellular molecules and determine the yields of processes induced by SE, particularly those driven by electrons of energy lower than around ~ 30 eV, which constitute the major portion of the SE energy distribution. Since the detrimental biological effects of ionizing radiation are usually caused by damage to the genome, most of the work related to LEE induced processes in biomolecules has been focused on DNA and its basic constituents [2].

At the theoretical level, there exists an obvious problem in treating electron scattering from DNA: the molecule is so large and complex that none of the conventional theoretical formulations are adequate to solve the electron-DNA interaction. These formulations are still limited to the treatment of relatively small molecules, usually composed of no more than a dozen atoms or so [28,29] and are therefore still far from that needed to understand electron scattering from most biological molecules (e.g., molecules such as DNA may contain up to 10^{10} atoms).

To solve the LEE-DNA scattering problem, a theoretical framework has recently been proposed [11,12] to describe LEE scattering from large biomolecules, having a helical topology. The problem was decoupled into two parts: first the electron interacts with the entire molecule and then the new wave functions, defined by the atomic arrangement within the molecule, interact at a specific site of the molecule (e.g., a basic subunit). This choice was dictated by the important contribution to the scattering cross sections arising from both resonances and electron diffraction at low energies; i.e., electron attachment requires the localization of the electron on a small subunit of the biomolecule and an electron of energy typically 5–15 eV has a wavelength that is of the order of molecular and intermolecular distances and is thus initially delocalized. In other words, the incident electron is first likely to undergo multiple intersite scattering before interacting at a specific site, where it can be captured in a resonant state. The simple model proposed consists of molecular subunits (i.e., bases, sugars, and phosphates) immersed in an optical potential U_{op} , which is constant between R -matrix shells, a working hypothesis used in the cross section calculations for simple molecules [30] and in the theory of low-

*Permanent address: Département de physique et Regroupement québécois sur les matériaux de pointe, Université de Sherbrooke, Sherbrooke, QC J1K 2R1, Canada.

energy electron diffraction in solids [31]. Due to the unavailability of scattering matrices for molecular subunits, the model was applied to scattering from the bases within DNA, which were represented by pseudomolecular units made of scattering centers.

We found important internal diffraction effects correlated to the average base pair distance along the helix of a *B*-type DNA like arrangement [11,12]. These patterns were resistant to disorder. However, in experiments on LEE scattering from DNA, the incoming electron first encounters the backbone before reaching the bases. Thus, to obtain a more adequate description of the LEE-DNA scattering problem, in the present work we added a pseudo-backbone (PB) linking the external edges of the pseudo base pairs (PBP). This allows us to calculate the influence of the PB on the internal diffraction patterns and to examine the effect of electron interference on backbone molecular subunits, for which experimental results [32–37] on resonance decay into the dissociative electron attachment (DEA) and dissociative excited state channels are available.

Furthermore, results on the desorption of OH⁻ induced by 0–19 eV electrons incident on self-assembled monolayer (SAM) films made of single and double DNA strands of different orientations with respect to a gold substrate have been recently reported [32]. Considering the availability to incoming electrons of OH containing DNA sites in the different orientations and configurations, the authors deduced that the OH⁻ signal arises from DEA to the phosphate unit of the backbone. However, their deduction assumes no change in electron capture probability by the phosphate group with the angle of incidence of the electron beam with respect to the axis of the DNA molecule. Considering the complexity of the DNA molecule, this assumption cannot be verified experimentally, whereas this sort of question can be answered with a relatively simple calculation as shown in this article.

We shall proceed, in the next section, with a brief recapitulation of the scattering model and its application to helical structures comprised of PBP and PB. In subsequent sections, the electron partial wave components on the phosphate group will be examined in an effort to characterize the effect of multiple scattering and the results will be discussed. We end with a conclusion.

II. MODEL

A. Multiple scattering theory

In Refs. [11,12], we presented the basic equations for multiple electron scattering within macromolecules, including DNA. For the latter, we proposed a simple model of molecular subunits (i.e., bases, sugars, and phosphates) immersed in an optical potential U_{op} , which is constant between their *R*-matrix shells (or between the muffin-tins), a working hypothesis that has been used in the calculations for simple molecules [30] and in the theory of low-energy electron diffraction in solids [31]. One can quite generally describe the scattering problem of a molecular subunit by its scattering matrix $S_{LL'}$, [24,38] where $L=(l,m)$ are the angular momentum quantum numbers. Each molecular subunit has an inci-

dent plane wave of momentum \vec{k} impinging on it plus the scattered waves of all other subunits. More specifically, we described the asymptotic form of the total wave function $\psi_{\vec{k}}^{(n)}(\vec{r})$ outside the *R*-matrix shell of a molecule centered at \vec{R}_n by the following equation:

$$\psi_{\vec{k}}^{(n)}(\vec{r}) = 4\pi e^{i\vec{k}\cdot\vec{R}_n} \sum_{LL'} i^l B_{\vec{k}L}^{(n)} Y_{L'}(\Omega_{\vec{r}}) \left[j_l(kr_n) \delta_{LL'} + \frac{1}{2} (S_{LL'} - \delta_{LL'}) h_{l'}^+(kr_n) \right], \quad (1)$$

where Y_L are spherical harmonics, j_l and $h_{l'}^+$ are the spherical Bessel function and Hankel function of the first kind, respectively, $\vec{r}_n = \vec{r} - \vec{R}_n$ and

$$B_{\vec{k}L}^{(n)} = Y_L^*(\Omega_{\vec{k}}) + \frac{1}{2} \sum_{n' \neq n} \sum_{L_1, L_2, L_2'} i^{l_1+l_2-l_2'} B_{\vec{k}L_2}^{(n')} (S_{L_2 L_2'}^{(n')} - \delta_{L_2 L_2'}) \times (-1)^{m_2'} e^{-i\vec{k}\cdot\vec{R}_{nn'}} F_{m_1, m_2, -m_2'}^{l_1, l_2, l_2'} Y_{L_1}(\Omega_{\vec{R}_{nn'}}) h_{l_1}^+(kR_{nn'}), \quad (2)$$

where

$$F_{m_1, m_2, m_3}^{l_1, l_2, l_3} = [4\pi(2l_1+1)(2l_2+1)(2l_3+1)]^{1/2} \times \begin{pmatrix} l_1 & l_2 & l_3 \\ 0 & 0 & 0 \end{pmatrix} \times \begin{pmatrix} l_1 & l_2 & l_3 \\ m_1 & m_2 & m_3 \end{pmatrix},$$

and $\begin{pmatrix} l_1 & l_2 & l_3 \\ m_1 & m_2 & m_3 \end{pmatrix}$ is the Wigner 3-*j* symbol [39], and $\vec{R}_{nn'} = \vec{R}_n - \vec{R}_{n'}$. Equation (2) implies a coupled set of linear equations for all $B_{\vec{k}L}^{(n)}$. As mentioned before [11,12], this would prove arduous if not impossible to solve were it not for the loss of coherence of the electrons due to inelastic collisions and to the presence of parasite scatterers (e.g., the structural water molecules in the grooves could be considered as such). These processes can be invoked through an imaginary part in the background optical potential U_{op} [31], i.e., an imaginary part to the electron wave number $\text{Im}(k) = \xi^{-1}$. Here ξ acts as a coherence length for the electrons. This representation allows approximate, though accurate, *local* solutions by truncated finite-size matrices containing the information for the number of subunits within a few coherence lengths. It is also exact for finite-sized segments.

B. Resonant capture

In an effort to extract physically meaningful information from the multiple scattering formalism, we had previously targeted a calculation of the capture amplitude $V_{\vec{k}}^{(c)}$ of an electron in a shape or core excited resonance of a basic subunit *C* positioned at \vec{R}_c . We had assumed a dominant capture channel symmetry corresponding to L_o and had used the one-center approximation of O'Malley [40] for the capture amplitude. When generalized to a multiple scattering situation, this led to

$$V_{\vec{k}}^{(c)} = \sqrt{4\pi} V_{L_o} [C_{\vec{k}L_o} + Y_{L_o}^*(\Omega_{\vec{k}})] e^{i\vec{k}\cdot\vec{R}_c}, \quad (3)$$

where

$$C_{\vec{k}L} = \frac{1}{2} \sum_{n' \neq C} \sum_{L_1, L_2, L_2'} i^{l_1+l_2-l_2'} B_{\vec{k}L_2}^{(n')} (S_{L_2L_2'}^{(n')} - \delta_{L_2L_2'}) (-1)^{m_2'} e^{-i\vec{k}\cdot\vec{R}_{Cn'}} \\ \times F_{m_1, m_2, -m_2'}^{l_1, l_2'} Y_{L_1}(\Omega_{\vec{R}_{Cn'}}) h_{l_1}^+(kR_{Cn'}) \quad (4)$$

and V_{L_o} is an energy and nuclear coordinate dependant amplitude. These equations are obtained by expanding the electronic wave function around \vec{R}_c .

We proposed a partial capture factor, which is in fact proportional to the square of the partial wave component of the total incoming wavefunction on the subunit at \vec{R}_c

$$\Gamma(L_o) = |\sqrt{4\pi} [C_{\vec{k}L_o} + Y_{L_o}^*(\Omega_{\vec{k}})]|^2, \quad (5)$$

and a relative partial capture factor $\Gamma_{\text{rel}}(L_o)$ which is Γ of Eq. (5) divided by its value without multiple scattering

$$\Gamma_{\text{rel}}(L_o) = |\sqrt{4\pi} [C_{\vec{k}L_o} + Y_{L_o}^*(\Omega_{\vec{k}})]|^2 / |\sqrt{4\pi} Y_{L_o}^*(\Omega_{\vec{k}})|^2. \quad (6)$$

These would serve as meaningful measures of the effect of multiple scattering on the capture probability in the L_o channel for both types of resonances.

III. SIMULATION

As before, our theory is specialized to a helical macromolecule made of repeating rung units (residues) of PBP and a backbone linking the external ends of the PBP that are constructed from centrosymmetric scatterers. The PBP are the same as in Refs. [11,12] and consists of planar PC and PG arrangement of scatterers resembling the cytosine-guanine (C-G) base pair unit of DNA [41]. The PB is composed of 11 scatterers on each side which are ordered to mimic the spatial arrangement of the sugar-phosphate units [41]. The resulting helix has a radius close to that of DNA [41]. The sum over n in Eq. (2) or (4) then runs over the individual scatterers. Moreover, for single centrosymmetric scatterers, one has $\frac{1}{2}(S_{LL'}^{(n')} - \delta_{LL'}) = i\delta_{LL'} e^{i\delta_{nl}} \sin(\delta_{nl})$, where δ_{nl} is the n th scatterer phase shift. We have used the phase shifts of Ar [42] for all scatterers as in our previous calculations.

The parameters of DNA were the following: a screw pitch of $c=3.4$ nm and a number of residues per turn $N_c=10$ which are characteristic of the B form of DNA, the $l=0, 1, 2$ phase shifts of the electronically inert species Argon, and a value of the wave function coherence length of 20 Bohr radii, that is $\xi=1.06$ nm. This value is representative of solids [31,42] and biological materials [43]; furthermore, it compensates for the artificial regularity of the helix.

IV. RESULTS AND DISCUSSION

A. Uniform helix

In our past work, we have chosen the incident direction to be perpendicular to the axis of helix. This choice had been

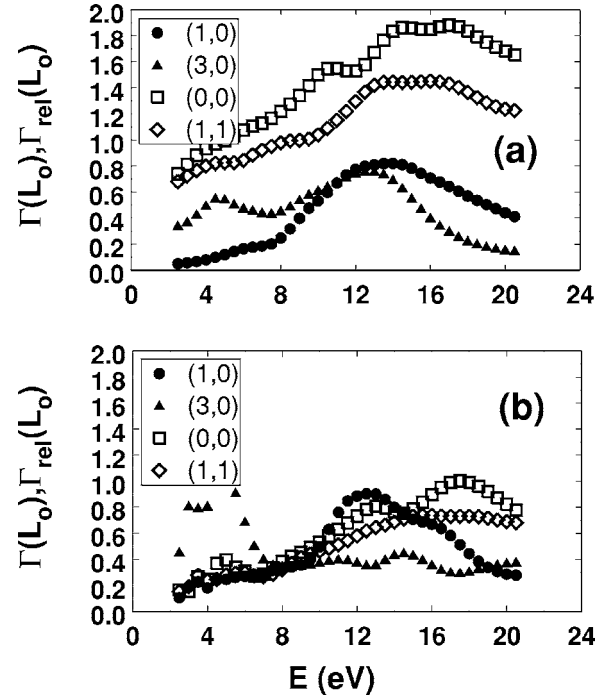


FIG. 1. Partial capture factors (a) without and (b) with a backbone, at the center of the PC ring as a function of electron energy relative to $\text{Re}(U_{\text{op}})$ using Ar phase shifts. Various entrance channels $L_o=(l_o, m_o)$ are shown. Γ is used for odd l_o+m_o channels and Γ_{rel} for even ones.

suggested by the experiments [1,2,5,8], in which the damage to DNA is measured for electrons impinging in a direction normal to a condensed film of the molecules. In such experiments, electrons are thus incident predominantly perpendicular to the DNA strands, which are expected to lie mostly in the plane of the films.

As was done in the previous publications, we calculated $\Gamma(L_o)$ and $\Gamma_{\text{rel}}(L_o)$ in Eqs. (5) and (6) in the middle of the PC ring for a few channels L_o . The results are plotted in Fig. 1. The magnitudes are generally smaller with the backbone, typically by a factor of 2, as illustrated by the (0,0) and (1,1) channels. The (1,0) channel, however, is as strong as without the backbone. The internal diffraction peaks are still observable. The backbone thus screens the base pairs to some extent while retaining their interference patterns.

Examination of the partial capture factors on the subunits of the backbone revealed a surprisingly large enhancement at low energy. In order to quantify this uniformly, we resort to a subsidiary quantity, the weighted partial capture factor

$$\Gamma_w(l_o) = \frac{\sum_{\vec{R}_C} \sum_{m_o} |\sqrt{4\pi} [C_{\vec{k}l_o m_o} + Y_{l_o m_o}^*(\Omega_{\vec{k}})] e^{i\vec{k}\cdot\vec{R}_C}|^2}{\sum_{\vec{R}_C} \sum_{m_o} |\sqrt{4\pi} Y_{l_o m_o}^*(\Omega_{\vec{k}}) e^{i\vec{k}\cdot\vec{R}_C}|^2}, \quad (7)$$

where the sum over \vec{R}_C runs over all subunits within a turn of the helix while the sum over m_o runs from $-l_o$ to l_o . Remember that the wave vector has an imaginary component so that the incident electron intensity is site dependent. The weighting factor in Eq. (7) (the denominator) has the extra property

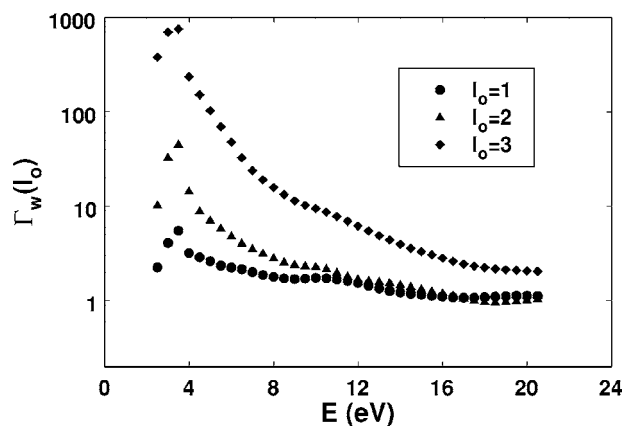


FIG. 2. Weighted partial capture factors at the center of the phosphate group on the backbone linking the PC rings as a function of electron energy relative to $\text{Re}(U_{\text{op}})$ using Ar phase shifts. Various entrance channels l_o are shown.

that it is independent of \hat{k} . This is advantageous when considering different incident directions, as in the following section. The results for the phosphate subunits bonded to the the PC ring side are shown in Fig. 2. There is a small signature of the internal diffraction pattern at 10–12 eV caused by the vertical piling of the PBP. The considerable enhancement is thus mostly due to constructive interference within the backbone itself. There are similar results, though of lesser amplitude, for the sugar subunits.

The results of Fig. 2 are of significance to our understanding of the mechanisms responsible for single strand breaks (SSBs) induced by LEEs, particularly below 5 eV. According to the recent results of Martin *et al.*, electrons of 0.1 to 4.5 eV can induce SSB in DNA but no double strand breaks (DSBs) [8]. Their SSB yield function exhibits two peaks at 0.8 and 2.2 eV, characteristic of the formation of transient anions near the energies of these peaks [8]. Owing to the low energy of these transient anion states, they were interpreted as shape resonances. Basically, the result of Martin *et al.* indicates that an electron localizes on a basic unit of DNA and subsequently this localization causes a SSB. A simple mechanism to explain this break would involve electron localization on the phosphate group of the backbone to produce a metastable $\text{P}=\text{O} \pi^*$ anion. According to the DFT calculation of Li *et al.* [15] crossing of the potential energy surface of this π^* state with the repulsive σ^* state of the same unit could break the $\text{P}-\text{O}$ bond of the backbone at the 3' or 5' position, if the transient anion is sufficiently long lived. In the model of Li *et al.* an electron was added to a short DNA strand composed of two sugar units linked together by a phosphate group. However, when a different model is used, consisting of a base linked to a sugar-phosphate unit different results are obtained as shown by the ab initio calculation of Simon's group [13,14]. Their data indicate that an electron initially captured by a base would transfer to the deoxyribose and unto the phosphate unit and then cause cleavage of the sugar-phosphate σ bond. Furthermore, a correlation exists between the results of Martin *et al.* and the magnitude and energies of transient anions formed below 5 eV in the gaseous bases which indicates that in

DNA SSB may occur via electron transfer from the bases [8,9]. On the other hand, recent studies of DEA to gaseous thymidine [44] show that an electron captured by thymine does not easily transfer to the sugar moiety.

Thus, there is presently considerable debate on the exact mechanism leading to SSB. The results of Fig. 2 indicate, however, that when a short chain of DNA is considered in a multiple electron scattering calculation, the probability of electron localization at the phosphate group is considerably higher than capture at other sites. In fact, the weighted partial capture factors at the center of phosphate groups can increase by orders of magnitude between 2 and 5 eV for certain partial waves. In other words, any dissociative transient anion state formed by electron capture at the phosphate group with a lifetime longer or of the order of the $\text{C}-\text{O}$ vibrations within DNA is expected to contribute significantly to SSB.

B. Orientation of DNA

In recent experiments on DNA films, Pan and Sanche [32] measured the desorption of OH^- stimulated by 0–14 eV electrons incident on films of self-assembled monolayers of the molecules. They found that when the axis of the DNA molecules lied parallel to the gold substrate, the OH^- signal was fivefold more intense than when the molecules lied perpendicular to the substrate. In view of these recent experimental results on short DNA segments lying parallel or perpendicular to a substrate, one wonders if it may not be differences in the interference enhancement for the two geometries that might explain the large differences in OH^- yields. In order to shed some light on this problem, we have performed simulations on a segment having 11 PBP. In the first calculation, the incident electron arrives perpendicular to the segment, at it would for segments lying horizontally on the substrate. In the second, it arrives in the axial direction as it would for segments vertically aligned on the substrate. We have used Eq. (7) with the sum over \vec{R}_C restricted to all phosphate subunits that are directly exposed to oncoming electrons for the horizontally aligned segments and to the two foremost exposed subunits, below the first PBP, in the vertical arrangement. We have labeled these quantities the surface partial capture factors $\Gamma_s(l_o)$. They are shown in Fig. 3.

Surprisingly, no significant difference is observed, in spite of totally different angles of incidence. We have checked this result by doing a run with an infinite coherence length. The same observation prevails. One can only conclude that the observed difference in OH^- yields does not come from differences in capture amplitudes. There is, however, a geometrical factor favoring the parallel orientation yield. There are approximately three times more phosphate groups per unit area of the film directly exposed to the incident electrons for the horizontal segments as compared to the vertical ones. This is insufficient to fully explain the large discrepancy in yields. One can therefore infer that the much lower yield of the vertical segments stems from the probable low diffusivity of the OH^- ions in the caged environment of the vertical segments.

V. CONCLUSION

DNA is a complex molecule which contains not only the bases and sugar and phosphate units as primary constituents

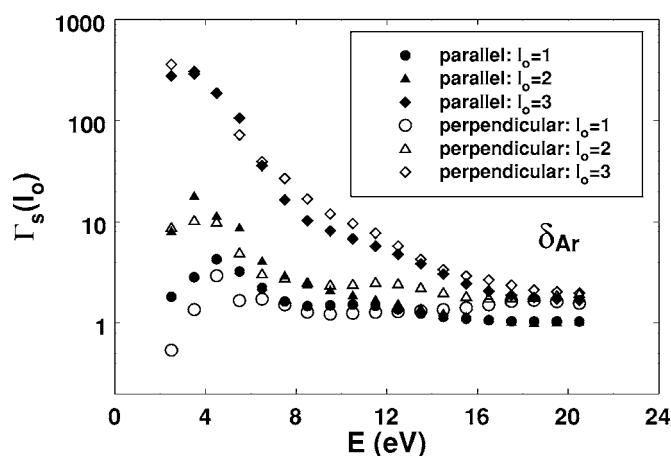


FIG. 3. Surface partial capture factors at the center of the phosphate groups as a function of electron energy relative to $\text{Re}(U_{op})$ using Ar phase shifts. Parallel and perpendicular segment orientations relative to the substrate are illustrated. Various entrance channels l_0 are shown.

but also structural water and ions. Thus, a precise description of LEE scattering from DNA must take into account all of these components and their arrangements. In our previous calculations, we considered the arrangement of the bases within DNA and its effect on the scattered electron wave functions. We addressed the multiple scattering problem and examined the various parameters that influence the coupling of the diffracted electron waves to electron states localized on the bases. The model allowed investigating *A*- and *B*-type DNA with and without introducing disorder in the bases. In practice, such disorder could be seen as due to pitch varia-

tions and the presence of H_2O and ions within the molecule which causes a loss of coherence in the diffracted partial waves.

As we are refining our theoretical model, more of the basic elements of DNA are introduced into our formulation. The added complexity not only provides a more adequate description of the phenomenon but allows one to analyze the effects of the different basic units on the scattered waves and the formation of transient anions. In this paper, we reported the results obtained when a backbone is added to the arrangement of the bases. Comparison of the partial electron capture factors with and without the backbone for various entrance channels shows that the probability of electron localization on the bases is generally smaller by typically a factor of 2 with the backbone. The diffraction patterns caused by the regular arrangement of the bases are retained in the presence of the backbone. On the other hand, the periodic repeated structure of the sugar-phosphate units of the backbone is not found to cause considerable diffraction features, but between 2–5 eV, electron localization at the phosphate unit is highly favored. Since SSB are believed to occur as a consequence of direct electron attachment or electron transfer to the phosphate group, this result could explain the high propensity of LEEs to induce SSB when compared to the damage caused by x rays [45]. Finally, calculations of electron capture factors at the phosphate group for electrons arriving parallel and perpendicular to the axis of DNA did not exhibit significant differences. This result indicates that differences observed experimentally in DNA damage due to different orientations of incoming electrons are not caused by variations of the diffracted wave amplitudes with angles of incidence.

- [1] B. Boudaïffa, P. Cloutier, D. Hunting, M. A. Huels, and L. Sanche, *Science* **287**, 1658 (2000).
- [2] L. Sanche, *Mass Spectrom. Rev.* **21**, 349 (2002).
- [3] A. Bass and L. Sanche, in *Charged Particle and Photon Interactions with Matter: Chemical, Physicochemical and Biological Consequences with Applications.*, edited by Y. Hatano and A. Mozumder (Marcel Dekker, New York, 2004).
- [4] H. Abdoul-Carime, S. Gohlke, and E. Illenberger, *Phys. Rev. Lett.* **92**, 168103 (2004).
- [5] X. Pan, P. Cloutier, D. Hunting, and L. Sanche, *Phys. Rev. Lett.* **90**, 208102 (2003).
- [6] A. M. Scheer, K. Aflatooni, G. A. Gallup, and P. D. Burrow, *Phys. Rev. Lett.* **92**, 068102 (2004).
- [7] T. Tanabe, K. Noda, M. Saito, E. B. Starikov, and M. Tateno, *Phys. Rev. Lett.* **93**, 043201 (2004).
- [8] F. Martin, P. D. Burrow, Z. Cai, P. Cloutier, D. Hunting, and L. Sanche, *Phys. Rev. Lett.* **93**, 068101 (2004).
- [9] S. Denifl, S. Ptasíńska, M. Probst, J. Hrušák, P. Scheier, and T. Märk, *J. Phys. Chem. A* **108**, 6562 (2004), see citations therein.
- [10] S. Ray, S. Daube, and R. Naaman, *Proc. Natl. Acad. Sci. U.S.A.* **102**, 15 (2005).
- [11] L. G. Caron and L. Sanche, *Phys. Rev. Lett.* **91**, 113201 (2003).
- [12] L. Caron and L. Sanche, *Phys. Rev. A* **70**, 032719 (2004).
- [13] J. Berdys, I. Anusiewicz, P. Skurki, and J. Simons, *J. Am. Chem. Soc.* **126**, 6441 (2004).
- [14] R. Barrios, P. Skurski, and J. Simons, *J. Phys. Chem. B* **106**, 7991 (2002).
- [15] X. Li, M. Sevilla, and L. Sanche, *J. Am. Chem. Soc.* **125**, 13668 (2003).
- [16] X. Li, M. Sevilla, and L. Sanche, *J. Phys. Chem. B* **108**, 5472 (2004), see citations therein.
- [17] F. Gianturco and R. Luccese, *J. Chem. Phys.* **120**, 7446 (2004).
- [18] F. Gianturco and R. Luccese, *J. Phys. Chem. A* **108**, 7056 (2004).
- [19] P. Mozejko and L. Sanche, *Radiat. Phys. Chem.* **73**, 77 (2005).
- [20] M. Inokuti, *Tech. Rep. TECDOC-799*, IAEA, 1995.
- [21] U. Uehara, H. Nikjoo, and D. Goodhead, *Radiat. Res.* **152**, 202 (1999).
- [22] J. LaVerne and S. Pimblott, *J. Phys. Chem.* **99**, 10540 (1995).
- [23] M. Inokuti, *Rev. Mod. Phys.* **43**, 297 (1971).
- [24] N. F. Mott and H. S. W. Massey, *The Theory of Atomic Collisions*, 3rd ed. (Clarendon, Oxford, 1965).
- [25] M. Bardiès and P. Pihet, *Cur. Pharm. Design* **6**, 1469 (2000).

- [26] A. Ahnesjö and M. Aspradakis, *Phys. Med. Biol.* **44**, R99 (1999).
- [27] *Research Needs and Opportunities in Radiation Chemistry Workshop*, DOE Final Report SC-0003, U.S. Department of Energy, 1998.
- [28] F. A. Gianturco and R. R. Lucchese, *J. Chem. Phys.* **108**, 6144 (1998).
- [29] M. H. F. Bettega, C. Winstead, and V. McKoy, *J. Chem. Phys.* **112**, 8806 (2000).
- [30] D. Dill and J. L. Dehmer, *J. Chem. Phys.* **61**, 692 (1974).
- [31] J. B. Pendry, *Low Energy Electron Diffraction* (Academic, London, 1974).
- [32] X. Pan and L. Sanche, *Phys. Rev. Lett.* **94**, 198104 (2005).
- [33] D. Antic, L. Parenteau, M. Lepage, and L. Sanche, *J. Phys. Chem.* **103**, 6611 (1999).
- [34] D. Antic, L. Parenteau, and L. Sanche, *J. Phys. Chem. B* **104**, 4711 (2000).
- [35] S. Ptasińska, S. Denifl, P. Scheier, and T. Märk, *J. Chem. Phys.* **120**, 8505 (2004).
- [36] M. Lepage, S. Letarte, M. Michaud, F. Motte-Tollet, M.-J. Hubin-Franskin, D. Roy, and L. Sanche, *J. Chem. Phys.* **109**, 5980 (1998).
- [37] S.-P. Breton, M. Michaud, C. Jäggle, P. Swiderek, and L. Sanche, *J. Chem. Phys.* **121**, 12240 (2004).
- [38] F. A. Gianturco and A. Jain, *Phys. Rep.* **143**, 347 (1986).
- [39] A. Messiah, *Quantum Mechanics* (Wiley, New York, 1962), Appendix C.
- [40] T. F. O'Malley and H. S. Taylor, *Phys. Rev.* **176**, 207 (1968).
- [41] R. L. P. Adams, J. T. Knowler, and D. P. Leader, *The Biochemistry of the Nucleic Acids*, 10th ed. (Chapman and Hall, New York, 1981).
- [42] M. Michaud, L. Sanche, C. Gaubert, and R. Baudoing, *Surf. Sci.* **205**, 447 (1988).
- [43] B. Boudaïfa, P. Cloutier, D. Hunting, M. A. Huels, and L. Sanche, *Radiat. Res.* **157**, 227 (2002).
- [44] S. Ptasińska, S. Denifl, P. Scheier, E. Illenberger, and T. Märk (unpublished).
- [45] In a direct comparison of the damage to DNA induced by LEEs and x rays during experiments performed under identical conditions, LEEs were found to be threefold more efficient to induce SSB for the same amount of energy deposited in dry multilayer DNA films. See Z. Cai, P. Cloutier, D. Hunting, and L. Sanche, *J. Phys. Chem. B* **109**, 4796 (2005).